WILEY InterScience® DISCOVER SOMETHING GREAT

PROTEINS STRUCTURE ■ FUNCTION ■ BIOINFORMATICS

Solvent effects in the slow dynamics of proteins

Konrad Hinsen[1,2]* and Gerald R. Kneller[1,2]

[1] Centre de Biophysique Moléculaire, CNRS UPR 4301, Rue Charles Sadron, 45071 Orléans Cedex 2, France

[2] Synchrotron Soleil, Saint Aubin, B.P. 48, 91192 Gif sur Yvette Cedex, France

ABSTRACT

The influence of solvent on the slow internal dynamics of proteins is studied by comparing molecular dynamics simulations of solvated and unsolvated lysozyme. The dynamical trajectories are projected onto the protein's normal modes in order to obtain a separate analysis for each of the associated time scales. The results show that solvent effects are important for the slowest motions (below $\approx$ 1 ps^{-1}) but negligible for faster motions. The damping effects seen in the latter show that the principal source of friction in protein dynamics is not the solvent, but the protein itself.

Proteins 2008; 70:1235–1242.

Key words: friction; normal modes.

INTRODUCTION

Protein–solvent interactions and the influence of solvent on a protein's thermodynamic properties have been the subject of many scientific investigations. For example, the importance of solvent in the stabilization of proteins is well recognized.[1] Dynamical aspects of protein–solvent interactions have been the subject of more recent studies. The influence of water and other solvents, including much more viscous solvents such as trehalose, on the dynamical or glass transition has been studied both experimentally and by simulation.[2,3,4,5,6] The terms "dynamical transition" and "glass transition" are used to describe the stronger-than-linear increase of atomic fluctuations with increasing temperature around 200 K. This effect is interpreted as the onset of anharmonic motions as the kinetic energy of the protein begins to exceed the energy barriers between conformational substates. However, this phenomenon is still more a thermodynamic than a dynamic one, because it concerns fluctuations amplitudes rather than relaxation effects with an associated time scale. This also holds for the observation that protein fluctuations[7] and protein folding[8] are "slaved" to solvent fluctuations.

In this article, we look at dynamical relaxation phenomena in the picosecond to nanosecond range in proteins and in particular at the influence of solvent on them. Compared to the fast vibrational dynamics observed by spectroscopic techniques, these are slow processes. However, processes that require transitions of important energy barriers, for example conformational transitions and folding or unfolding, are even much slower.

In the context of theoretical models and simulation techniques, a major motivation for studying protein–solvent interactions has been the wish to avoid explicit solvent models because of their complexity and significant CPU time costs. The most important effort has gone into modeling the energetic impact of solvent by continuum solvent and Poisson–Boltzmann models,[9] but the dynamic influence of solvent has also been considered in approaches based on Langevin and Brownian dynamics.[10,11] Langevin and Brownian dynamics were originally developed for large particles suspended in a liquid with the assumption that the interactions of the particles with the molecules of the liquid can be described by random collisions. These random collisions drain energy from the drift motions of the suspended particles through friction, but also act as a heat bath that supplies energy back to the particles. In Langevin and Brownian dynamics applied to proteins, the protein atoms take the role of the suspended particles and the solvent is identified with the liquid that acts as a heat bath and a source of friction. This implies that friction in proteins is a solvent effect, an assumption that is also often stated explicitly (see e.g.[10,12,13]). However, to our knowledge there is no theoretical or

*Correspondence to: Konrad Hinsen, Centre de Biophysique Moléculaire, CNRS UPR 4301, Rue Charles Sadron, 45071 Orléans Cedex 2, France. E-mail: hinsen@cnrs-orleans.fr
Received 2 March 2007; Revised 5 June 2007; Accepted 6 June 2007
Published online 12 September 2007 in Wiley InterScience (www.interscience.wiley.com). DOI: 10.1002/prot.21655

experimental basis for this hypothesis. On the contrary, analysis of Molecular Dynamics (MD) simulations has shown that the principal source of friction in a protein is the protein itself.[14]

In this work, we use computer simulations of solvated and unsolvated lysozyme, as well as of water, to investigate the dynamical relation of protein and solvent. We look at projections of the MD trajectories onto the protein's normal modes in order to study solvent effects at different time and length scales, and we discuss the implications for the use of stochastic simulation techniques for proteins.

MOLECULAR DYNAMICS AND NORMAL MODES

To analyze the impact of the presence of solvent on the internal dynamics of lysozyme, we have performed two MD simulations and a normal mode calculation for lysozyme. The starting point was in all cases the experimental structure of hen-egg lysozyme obtained by Vaney *et al.*[15] and available from the Protein Data Base[16] under the code 193L. All calculations were performed using the simulation library MMTK[17] and the Amber94 force field,[18] which implies the use of the TIP3P model for water of which we use the flexible form as defined by the Amber94 parameter files.

For the first MD simulation, one lysozyme molecule was equilibrated together with 3403 water molecules in an orthogonal box with periodic boundary conditions in an NpT ensemble at a temperature of 300 K and a pressure of 1 atm. After an equilibration period of several nanoseconds, up to stabilization of the system volume, a simulation of 1.5 ns was performed for analysis. The NpT ensemble was realized using the extended systems method implemented in a Velocity–Verlet algorithm, [19,20,21] with relaxation time parameters of 0.2 ps for the thermostat and 1.5 ps for the barostat. The integration time step was 1 fs, but only every 40th step was stored in a trajectory file, leading to a sampling step size of $\Delta t = 0.04$ ps. According to Shannon's theorem, our trajectory thus contains motions up to a frequency of 12.5 ps^{-1} ($\approx$400 cm^{-1}) but no faster ones.

The choice of the NpT ensemble and of the simulation length of 1.5 ns was motivated by the possibility to verify our simulation by comparison with neutron scattering data obtained at constant temperature and pressure and using an instrument whose energy resolution is of the same order of magnitude as that of the trajectory.[22] As the slowest vibrational motion in lysozyme happens on a time scale of 6 ps, a 1.5 ns trajectory provides sufficient sampling. The extended systems method implements the NpT ensemble through purely deterministic dynamics, that is without adding stochastic elements that could add friction to the system.

For the second MD simulation, lysozyme was equilibrated in vacuum at constant temperature (300 K). The other simulation parameters are identical to those of the first simulation.

We also generated a pure solvent trajectory of a length of 700 ps for a box containing 500 water molecules equilibrated at a temperature of 300 K and a pressure of 1 atm, using the same parameters as for the lysozyme trajectories.

For the normal mode calculation, an energy minimization was performed for lysozyme in vacuum using a steepest-descent algorithm initially and a conjugent-gradient minimizer for the final part. The minimization was continued until the energy gradient was smaller than 10^{-3} kJ/mol/nm. A standard vibrational normal mode calculation (diagonalization of the Hessian in mass-weighted coordinates) was then performed, resulting in a set of orthonormal normal mode vectors $\tilde{\mathbf{u}}_k$ ($k = 1 \ldots 3N$) and corresponding vibrational frequencies ν_k. Here and in the following, a tilde indicates mass-weighted coordinates.

Since we are interested in the internal dynamics of lysozyme, and not in its diffusional motion inside the water box, we removed the global diffusion from the trajectory of solvated lysozyme prior to any further analysis. This was achieved by replacing the lysozyme conformation at each time step by its optimal superposition[23] onto the initial configuration.

We then calculated the projections of the two MD trajectories onto the normal modes of lysozyme.[24] First we determined the linear transformations that superpose the average conformation of each trajectory onto the minimized conformation for which the normal modes were obtained. These transformations were applied to each time step in order to obtain the normal-mode aligned trajectories $\mathbf{R}^{(s)}(n\Delta t)$ (solvated lysozyme) and $\mathbf{R}^{(v)}(n\Delta t)$ (lysozyme in vacuum), where n enumerates the time steps and $\mathbf{R}$ is a $3N$-dimensional vector comprising the positions of the N atoms in the protein. The projections on the modes are then obtained as

$$c_k^{(s/v)}(n\Delta t) = (\tilde{\mathbf{R}}^{(s/v)}(n\Delta t) - \tilde{\mathbf{R}}_{av}^{(s/v)}) \cdot \tilde{\mathbf{u}}_k, \qquad (1)$$

where $\tilde{\mathbf{R}}_{av}^{(s/v)}$ is the average conformation of each trajectory. The projections contain the same information as the trajectories themselves, which can in fact be reconstructed through

$$\tilde{\mathbf{R}}^{(s/v)}(n\Delta t) = \tilde{\mathbf{R}}_{av}^{(s/v)} + \sum_{k=1}^{3N} c_k^{(s/v)}(n\Delta t)\tilde{\mathbf{u}}_k. \qquad (2)$$

This follows from the fact that the normal mode vectors $\tilde{\mathbf{u}}_k$ are an orthonormal basis of the $3N$-dimensional coordinate space. The projections $c_k^{(s/v)}$ thus describe the conformation of the protein in a coordinate system defined

 DOI 10.1002/prot

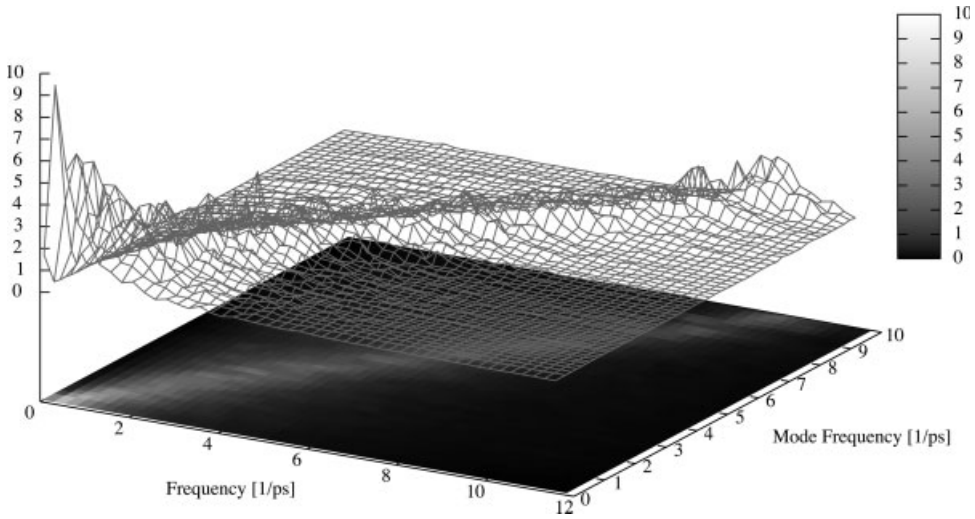

Figure 1

The frequency spectrum of the velocity autocorrelation function of the mode-projected coordinates as a function of the mode frequency for solvated lysozyme.

by the normal modes, whereas the positions $\mathbf{R}^{(s/v)}$ describe the conformation in a $3N$-dimensional Cartesian coordinate system. It follows that the time derivatives $\dot{c}_k^{(s/v)}$ are the normal-mode based velocity coordinates.

We note that in Eq. (1), we have chosen to use the average structure as the reference for the calculation of the normal mode projections. We could as well have chosen the minimized structure for which the normal modes were calculated. Our choice of the average structure is motivated by the fact that it minimizes the extreme values of $c_k^{(s/v)}(n\Delta t)$. Considering that normal modes describe small motions around a stable structure, this is more important than using the same reference structure for the trajectory and the normal mode calculations, as the collective normal modes are known to be unsensitive to small changes in the configuration.

To characterize the dynamics of solvated and unsolvated lysozyme at different time scales, we calculated the velocity autocorrelation function $\psi_k^{(s/v)}(n\Delta t)$, defined by

$$\psi_k^{(s/v)}(t) = \left\langle \dot{c}_k^{(s/v)}(t)\dot{c}_k^{(s/v)}(0) \right\rangle, \qquad (3)$$

and its frequency spectrum, the density of states

$$g_k^{(s/v)}(\omega) = \int_0^\infty dt\, \cos(\omega t)\, \psi_k^{(s/v)}(t), \qquad (4)$$

for each mode $k = 1 \ldots 3N$ using autoregressive models for the velocities $\dot{c}_k^{(s/v)}$,[25] which is equivalent to the maximum entropy method. We used autoregressive models of order $P = 1000$ and the smallest possible sampling step size, $\Delta t = 0.04$ ps. We also calculated the mean-square displacement (MSD) $W_k^{(s/v)}(n\Delta t)$, defined by

$$W_k^{(s/v)}(t) = \left\langle \left[c_k^{(s/v)}(t) - c_k^{(s/v)}(0) \right]^2 \right\rangle, \qquad (5)$$

for each mode projection using an efficient FFT-based algorithm.[26]

The velocity autocorrelation functions can be summed over all modes yielding, up to a constant prefactor, the standard mass-weighted average atomic velocity autocorrelation function:

$$\sum_{k=1}^{3N} \psi_k^{(s/v)}(n\Delta t) = \sum_{j=1}^{N} \left\langle \dot{\tilde{\mathbf{R}}}_j^{(s/v)}(n\Delta t) \cdot \dot{\tilde{\mathbf{R}}}_j^{(s/v)}(0) \right\rangle \qquad (6)$$

A similar relation holds for the spectra because of the linearity of the Fourier transform.

MODE-PROJECTED DYNAMICS

For a first overview of the mode-projected dynamics, we show the frequency spectrum for each mode projection for solvated lysozyme in a 3D graph (Fig. 1). This graph clearly shows that the frequency spectrum for each mode has a maximum near the vibrational frequency of that mode. It also shows that for the higher mode frequencies (above 2 $ps^{-1} \approx 70\ cm^{-1}$), the structure of the spectrum is rather simple: a symmetric distribution about the maximum. For the lower mode frequencies, the spectrum has a more complex and less symmetric form. Looking at the difference between the spectra for solvated

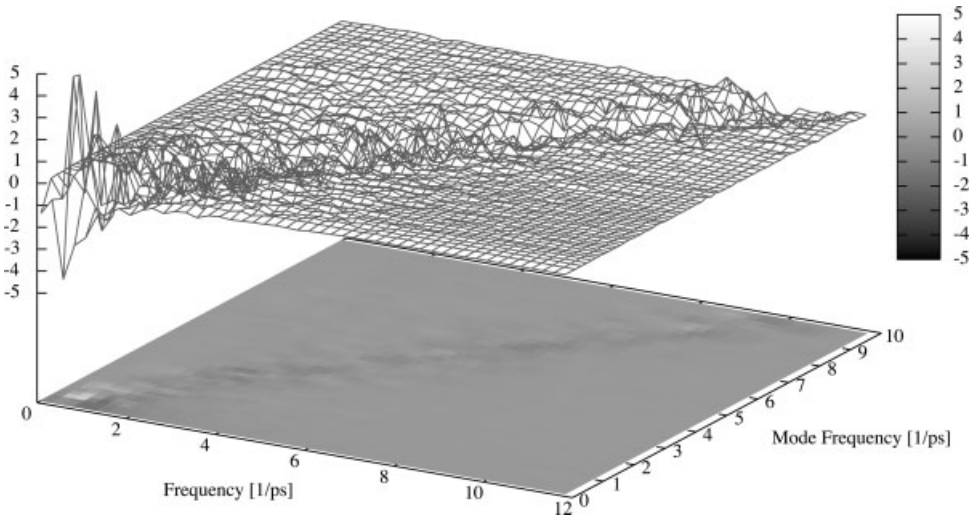

Figure 2

The difference of the frequency spectra for solvated and unsolvated lysoyme as a function of the mode frequency. The scale is the same as in Figure 1.

and unsolvated lysozyme (Fig. 2), we see that the difference is very small above 2 ps^{-1} but rather important for lower mode frequencies. Both observations suggest that there are two different dynamic regimes, which we will discuss separately. We will discuss the high-frequency regime first because it is simpler.

High-frequency regime

Considering that the sampling interval of our trajectories imposes an upper frequency limit of 12.5 ps^{-1} for our analyses, the high-frequency regime that we observe actually belongs to the lower-frequency motions of a protein, whose total vibrational frequency spectrum extends up to 100 ps^{-1}. In the following discussion, we look at normal modes whose frequencies range from 2 to 8 ps^{-1}. All of these modes describe motions on the length scales of secondary structure elements. At 2 ps^{-1}, we see deformations and dislocations of α-helices and loops, whereas 8 ps^{-1} corresponds to deformations of the ends of helices and of the surrounding peptide chain segments that link the helices to neighbouring secondary structure motifs.

Figure 3 shows the velocity autocorrelation function of the mode-projected trajectories, both for solvated and for unsolvated lysozyme. Each curve corresponds to a single mode in the frequency range 2–8 ps^{-1}. Figure 4 shows the corresponding frequency spectra (the same data as in Fig. 1), with vertical lines indicating the frequencies of the modes. To remove excessive noise in the spectra, they have been smoothed by replacing each data point by its average with its two neighbors. As it was already mentioned above, the spectra show clearly that the dominant frequency for each mode projection is the vibrational frequency of the mode. However, all spectra have nonvanishing contributions at low frequencies down to zero. These contributions are caused not only by couplings to slower vibrational modes due to anharmonicities in the potential, but also by slow diffusional motions that result from transitions between multiple vibrational substates.

Comparing the correlation functions and spectra for solvated and unsolvated lysozyme, we note in particular their remarkable similarity. There seems to be a slightly stronger damping in the vacuum simulation at 4 ps^{-1} and beyond, but the difference is probably not signifi-

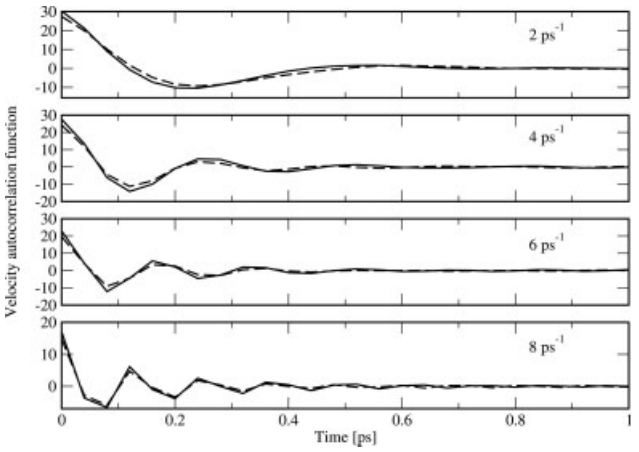

Figure 3

The velocity autocorrelation function of the mode-projected coordinates for four different modes whose vibrational frequencies are, respectively, 2, 4, 6, and 8 ps^{-1}. The curves for solvated lysozyme are drawn out, the ones for lysozyme in vacuum are dashed.

DOI 10.1002/prot

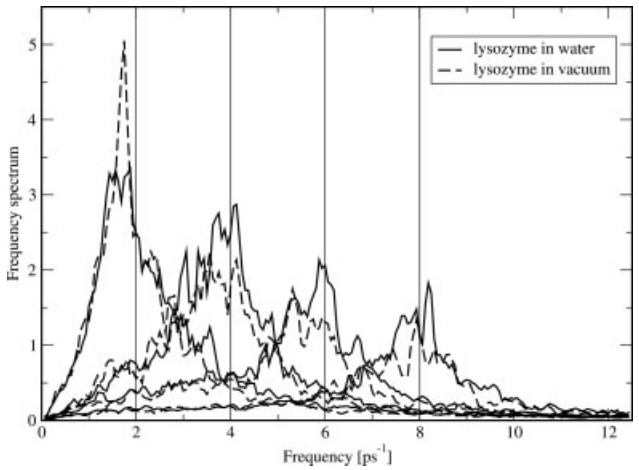

Figure 4

The frequency spectrum of the velocity autocorrelation function of the mode-projected coordinates for four different modes whose vibrational frequencies are, respectively, 2, 4, 6, and 8 ps^{-1}. The curves for solvated lysozyme are drawn out, the ones for lysozyme in vacuum are dashed. The vertical lines indicate the vibrational frequencies of the four modes.

cant, considering that neither trajectory is long enough to ensure sufficient sampling of the protein's configuration space. At 2 ps^{-1}, the solvated lysozyme shows slightly higher damping, marking the transition to the low-frequency regime that will be discussed later.

We thus find that the internal dynamics of both solvated and unsolvated lysozyme in this regime is characterized by damped vibrations. The strong similarity between solvated and unsolvated lysozyme indicates that the damping has its origin inside the protein itself, and not in the solvent as is frequently assumed. We also note a nonvanishing diffusional contribution to the motions in this regime.

Low-frequency regime

At the lower end of the frequency spectrum of a protein, we find the modes that describe the large-scale motions that are specific to each protein, that is motions that deform the tertiary and quaternary structure. In the case of lysozyme, the first three modes describe the relative motions of the two dynamic domains.[27]

The velocity autocorrelation function and its frequency spectrum for the projections onto the first three modes are shown in Figure 5. In unsolvated lysozyme, we see weakly damped oscillations, as in the high-frequency regime. However, these motions become overdamped in the presence of water. For the slowest modes, the solvent is thus the most important source of friction.

Mean-square displacements

Until now, we have looked at the velocity autocorrelation functions and their frequency spectra, that is quantities that describe the relaxation of velocity fluctuations due to friction effects. Another quantity of interest is the MSD $W(t)$, which measures how far (on average) the system moves away from its original configuration in a given amount of time. In a liquid, the MSD grows linearly with time (except for very short times), with the slope defining the diffusion constant. In a system that cannot move arbitrarily far away from its initial configuration, the MSD approaches an asymptotic value which is equal to twice the mean-square fluctuations. This is the case for the internal motions of a protein that we are interested in.

The MSD and the velocity autocorrelation function are related through

$$W_k^{(s/v)}(t) = 2\int_0^t \mathrm{d}t'\,(t-t')\,\psi_k^{(s/v)}(t'), \qquad (7)$$

$$\psi_k^{(s/v)}(t') = \frac{1}{2}\frac{\mathrm{d}^2}{\mathrm{d}t^2}\,W_k^{(s/v)}(t). \qquad (8)$$

The velocity autocorrelation function is thus more sensitive to fast motions, whereas the MSD is more sensitive to slow motions. This can be seen most easily in frequency space, where a time derivative corresponds to a multiplication with $i\omega$. The importance of slow motions for the MSD can also be seen from its relation to the frequency spectrum of the velocity autocorrelation function, which includes a factor $1/\omega^2$:

$$W_k^{(s/v)}(t) = \frac{4}{\pi}\int_0^\infty \mathrm{d}\omega\,\frac{1-\cos\omega t}{\omega^2}\,g_k^{(s/v)}(\omega). \qquad (9)$$

The sensitivity to slow motions also means that much longer simulations are required in order to obtain con-

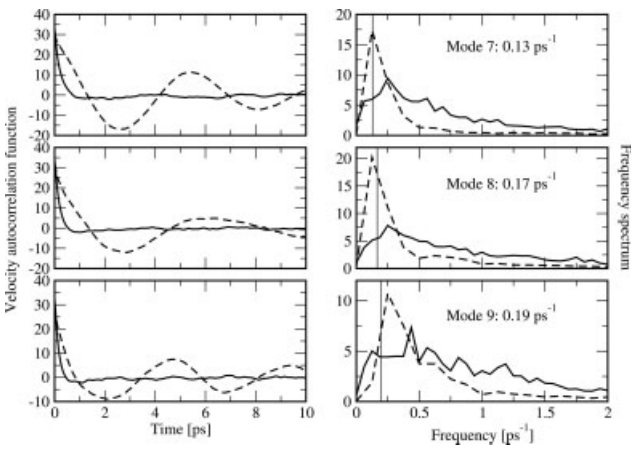

Figure 5

The velocity autocorrelation function (left) and its frequency spectrum (right) of the mode-projected coordinates for the first three non-zero modes (top to bottom). The curves for solvated lysozyme are drawn out, the ones for lysozyme in vacuum are dashed. The vertical lines in the right-hand column indicate the vibrational frequencies of the three modes.

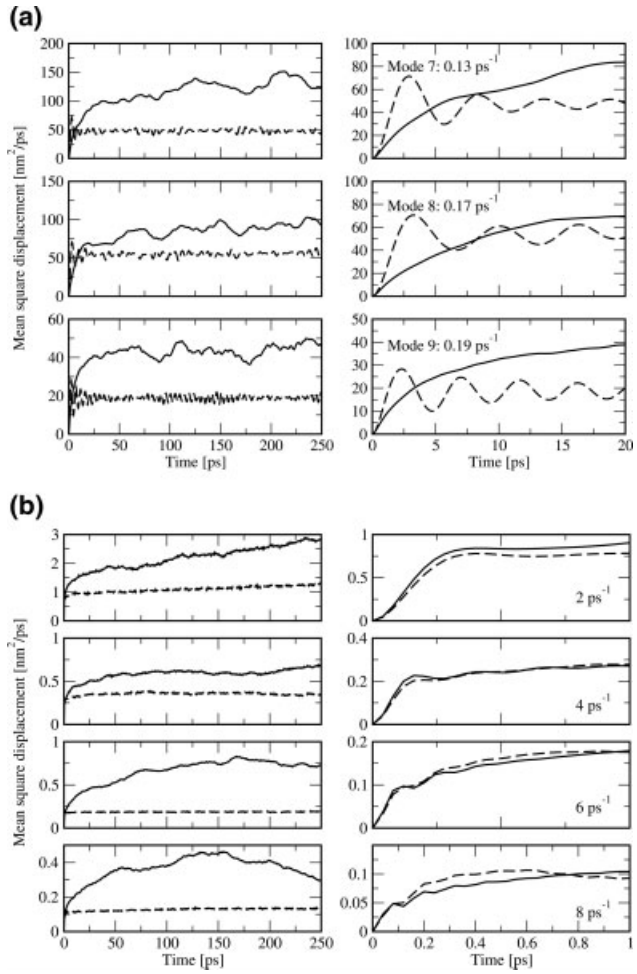

Figure 6

*The MSD of the mode-projected trajectories for the first three modes (**a**) and for four different modes whose vibrational frequencies are, respectively, 2, 4, 6, and 8 ps^{-1} (**b**). The curves for solvated lysozyme are drawn out, the ones for lysozyme in vacuum are dashed. The plots on the right are zoom views into the plots on the left showing the short-time behavior. As explained in section "mean-square displacement", the trajectories are too short to obtain reliable long-time values for the MSD, but the differences are nevertheless of interest.*

vergence for the MSD. Our simulations for solvated lysozyme (as in fact most, if not all, MD simulations of proteins in solution that have been published) are not long enough to obtain convergence except for very short times, as can be seen from the fact that the MSD does not reach a plateau value. Nevertheless, a comparison of the trajectories of solvated and unsolvated lysozyme is possible and of interest.

The MSD for solvated and unsolvated lysozyme are shown in Figure 6(a) (for the first three modes) and Figure 6(b) (modes at 2, 4, 6, and 8 ps^{-1}). The plots on the left show the MSD up to 250 ps, that is for times at which the velocity autocorrelation function is already negligibly small. The plots on the right show a zoom into the short-time behavior, which mostly confirms the observations on the velocity autocorrelation functions.

The most striking feature in Figure 6(a) is that the MSD for lysozyme in vacuum shows a rapid increase to a plateau value, modulated by initial oscillations. This is the characteristic shape for a damped oscillator. It indicates that the motion is restricted to the surroundings of a single stable conformation, that is there are no conformational transitions along the coordinates described by the first three modes. For solvated lysozyme, the MSD grows steadily and reaches larger values, indicating conformational transitions due to diffusive motion. However, on the time scale we are looking at, the difference in the MSD is not very important, meaning that the number of conformational substates visited is still quite small. The short-time zoom shows that the diffusive motion is controlled by the solvent, as has already been observed in the velocity autocorrelation function.

The projections on the higher-frequency modes shown in Figure 6(b) show a similar difference between the dynamics of the solvated and the unsolvated protein: in the presence of solvent, there are more conformational transitions. However, the dynamics of both systems is diffusive, and the similarity in the short-time plots shows that the friction effects that cause the diffusive motions have their origin inside the protein, as has already been seen from the velocity autocorrelation functions.

DISCUSSION

Summarizing our observations from the previous sections, we note that (1) the major source of friction is the protein, not the water, (2) the solvent becomes the major source of friction for a few very slow modes, and (3) the presence of water facilitates the transitions between conformational substates.

To understand why the dynamic influence of water is limited to the low-frequency regime, we need to consider two different aspects: (1) Why is the solvent influence so small for mode frequencies above 2 ps^{-1}? (2) Why is there such an important influence for the slowest motions?

To answer the first question, we have to look at the origin of friction in molecular systems. At the macroscopic scale of materials, friction is caused by the roughness of surfaces sliding against each other. In a molecular system, it is the roughness of effective potential energy surfaces that causes friction. We illustrate this in Figure 7. The ideal harmonic potential energy surface would lead to a perfect vibrational motion. However, coupling to faster motions introduce energy barriers that cause friction. These faster motions include local conformational changes (e.g. rotations of methyl groups) and collisions between sidechains. Considering that the mass density in a protein is about twice the density of water, it should be

DOI 10.1002/prot

expected that the protein itself is a more important source of friction than the surrounding water molecules. Moreover, the effect of the latter is limited to the protein surface. In fact, we have shown earlier[14] in a residue-by-residue analysis of friction in a protein that the single-atom friction coefficient is proportional to the mass density in the immediate environment of the atom, and thus higher inside the protein than near the surface.

It is only the slowest modes in a protein that involve little deformation of the interior, and thus little friction originating in the protein itself. However, these modes change the shape of the protein and thereby its surface, making interactions with the surrounding water molecules more important. Moreover, as Figure 8 shows, the frequency spectrum of the velocity autocorrelation function of water has its maximum at 1.36 ps^{-1}, that is in the low-frequency regime discussed earlier.

Ideally, one would verify this explanation by calculating the friction constants for the mode-projected trajectories. If our explanation is right, the friction constants for solvated and unsolvated lysozyme should be very similar for most of the modes, with only the lowest modes showing a marked increase of friction due to the solvent. Unfortunately, the long-time memory effects in protein dynamics (see e.g.[22,28]) make it practically impossible to calculate meaningful friction constants from MD trajectories. We will discuss this problem in a separate publication.

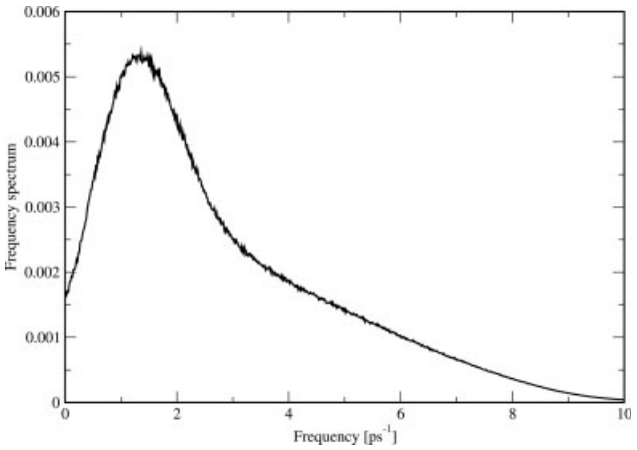

Figure 8

The frequency spectrum of the velocity autocorrelation function of water.

CONCLUSION

Our comparison of the internal dynamics of solvated and unsolvated lysozyme has shown that the dynamical influence of solvent is significant only for the slowest motions of the protein. These motions being the functionally relevant ones, the impact of solvation is of course far from negligible. However, the widespread notion that friction and damping are caused by the solvent (see e.g.[10,12,13]) is wrong. The dynamics of lysozyme in vacuum are already strongly damped, the principal source of friction is thus clearly the protein itself.

Much earlier studies (e.g.[29,30]) on single-atom dynamics in proteins have already noted that solvent effects on friction in proteins are small except at the surface. However, the relaxation times of single-atom dynamics are much shorter than those of any of the motions we consider here. A study on melittin published in 1991 by Kitao *et al.*[31] and a subsequent similar study on BPTI by Hayward *et al.*[32] are more similar to our work in looking at the projections of MD trajectories on collective coordinates. However, due to the computational limitations of the time, neither of these studies permits a conclusion that could be generalized to compactly folded proteins: melittin is too small to have a tertiary structure, and the BPTI trajectories were too short to sample the relaxation processes of the collective motions.

Our findings also have important practical consequences for the application of stochastic methods to the simulation of protein dynamics. In stochastic models, the friction constants must be chosen to represent mainly the friction because of the protein (see e.g.[14]). This is the opposite of what is habitually done in Langevin and Brownian Dynamics simulations, where friction coefficients are chosen to be proportional to a particle's solvent-exposed surface (e.g.[10,33]) or all particles are considered fully immersed into solvent (e.g.[11,34,35]), the idea always being that friction is a solvent effect. How-

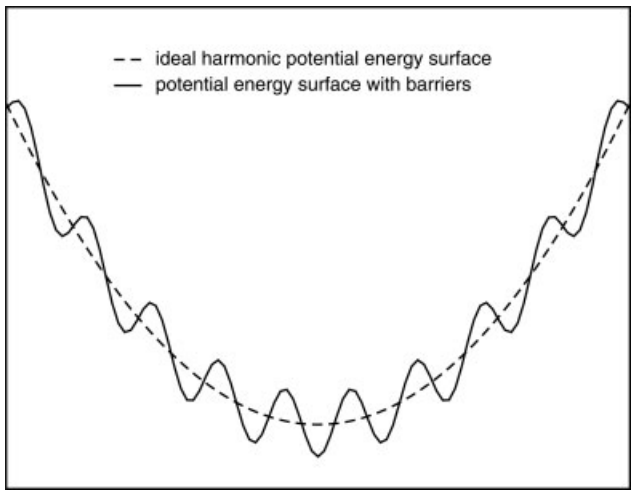

Figure 7

An ideal harmonic potential energy surface and a more realistic surface with many small barriers. The barriers are caused by couplings to faster motions such as collisions between sidechains.

ever, the long-time memory effects in protein dynamics[22,28] pose the even more fundamental question if simulation techniques based on Markov processes are adequate at all. It may be necessary to develop non-Markovian techniques that use a memory function instead of a friction constant to describe the friction effects in a protein correctly. It may also be necessary to take the correlations between the atoms into account by using a nondiagonal memory matrix.

The time scale that we have considered in this work is the lower end of the range that describes motions around a stable conformation. These are in general not the slowest motions in a protein. Transitions between significantly different conformations as well as unfolding and refolding happen on much longer time scales. It is to be expected that the dynamics of these motions are dominated by the solvent dynamics[7,8]; in fact, many of them do not occcur at all in vacuum. The interplay of the intrinsic protein dynamics that we have looked at in this study and the solvent-mediated dynamics of much slower processes remains to be studied in the future.

REFERENCES

1. Timasheff SN. Solvent effects on protein stability. Curr Opin Struct Biol 1992;2:35–39.
2. Cordone L, Ferrand M, Vitrano E, Zaccai G. Harmonic behaviour of trehalose-coated carbon-monoxy-myoglobin at high temperature. Biophys J 1999;76:1043–1047.
3. Tarek M, Tobias DJ. Role of protein–water hydrogen bond dynamics in the protein dynamical transition. Phys Rev Lett 2002;88: 138101.
4. Tournier AL, Xu J, Smith JC. Translational hydration water dynamics drives the protein glass transition. Biophys J 2003;85:1871–1875.
5. Gabel F, Weik M, Doctor BP, Saxena A, Fournier D, Brochier L, Renault F, Masson P, Silman I, Zaccai G. The influence of solvent composition on global dynamics of human butyrylcholinesterase powders: a neutron-scattering study. Biophys J 2004;86:3152–3165.
6. Kurkal V, Daniel RM, Finney JK, Tehei M, Dunn RV, Smith JC. Low frequency enzyme dynamics as a function of temperature and hydration: a neutron scattering analysis. Chem Phys 2005;317:267–273.
7. Fenimore PW, Frauenfelder H, McMahon BH, Parak FG. Slaving: solvent fluctuations dominate protein dynamics and functions. Proc Nat Acad Sci USA 2002;99:16047–16051.
8. Frauenfelder H, Fenimore PW, Chen G, McMahon BH. Protein folding is slaved to solvent motions. Proc Nat Acad Sci USA 2006;103:15469–15472.
9. Feig M, Brooks CL. Recent advances in the development and application of implicit solvent models in biomolecule simulations. Curr Opin Struct Biol 2004;14:217–224.
10. Lamm G, Szabo A. Langevin modes of macromolecules. J Chem Phys 1986;85:7334–7348.
11. Hamelberg D, Shen T, McCammon JA. Insight into the role of hydration on protein dynamics. J Chem Phys 2006;125:094905.
12. Venable R, Pastor RW. Frictional models for stochastic simulations of proteins. Biopolymers 1988;27:1001–1014.
13. Ma J. Usefulness and limitations of normal mode analysis in modeling dynamics of biomolecular complexes. Structure 2005;13:373–380.
14. Hinsen K, Petrescu AJ, Dellerue S, Bellissent-Funel MC, Kneller GR. Harmonicity in slow protein dynamics. Chem Phys 2000;261(1/2):25–37. Special Issue "Condensed phase structure and dynamics: a combined neutron scattering and molecular modelling approach".
15. Vaney MC, Maignan S, RiesKautt M, Ducruix A. High-resolution structure (1.33 Å) of a HEW lysozyme tetragonal crystal grown in the APCF apparatus. Data and structural comparison with a crystal grown under microgravity from spacehab-01 mission. Acta Cryst D Biol Cryst 1996;52:505–517.
16. Berman HM, Westbrook J, Feng Z, Gilliland G, Bhat TN, Weissig H, Shindyalov IN, Bourne PE. The protein data Bank. Nucl Acids Res 2000;28:235–242.
17. Hinsen K. The molecular modeling toolkit: a new approach to molecular simulations. J Comput Chem 2000;21:79–85.
18. Cornell WD, Cieplak P, Bayly CI, Gould IR, Merz KM Jr, Ferguson DM, Spellmeyer DC, Fox T, Caldwell JW, Kollman PA. A second generation force field for the simulation of proteins and nucleic acids. J Am Chem Soc 1995;117:5179.
19. Allen MP, Tildesley DJ. Computer simulation of liquids. Oxford University Press: Oxford; 1987.
20. Andersen H. Molecular dynamics at constant pressure and/or constant temperature. J Chem Phys 1980;72:2384–2393.
21. Nosé S. A unified formulation of the constant temperature molecular dynamics methods. J Chem Phys 1084;81:511–519.
22. Calandrini V, Hamon V, Hinsen K, Calligari P, Bellissent-Funel M-C, Kneller GR. Relaxation dynamics of lysozyme in solution under pressure: Combining molecular dynamics simulations and quasielastic neutron scattering. Chem Phys, in press; doi:10.1016/j.chemphys.2007.07.018.
23. Kneller GR. Superposition of molecular structures using quaternions. Mol Simul 1991;7:113–119.
24. Horiuchi T, Go N. Projection of monte carlo and molecular dynamics trajectories onto the normal mode axes: Human lysozyme. Proteins 1991;10:106–116.
25. Kneller GR, Hinsen K. Computing memory functions from Molecular Dynamics simulations. J Chem Phys 2001;115:11097–11105.
26. Rog T, Murzyn K, Hinsen K, Kneller GR. nMoldyn: A Program Package for a Neutron Scattering Oriented Analysis of Molecular Dynamics Simulations. J Comput Chem 2003;24:657–667.
27. Hinsen K. Analysis of domain motions by approximate normal mode calculations. Proteins 1998;33:417–429.
28. Kneller GR, Hinsen K. Fractional brownian dynamics in proteins. J Chem Phys 2004;121:10278–10283.
29. van Gunsteren WF, Karplus M. Protein dynamics in solution and in a crystalline environment: a molecular dynamics study. Biochemistry 1982;21:2259–2274.
30. Swaminathan S, Ichiye T, van Gunsteren W, Karplus M. Time dependence of atomic fluctuations in proteins: analysis of local and collective motions in bovine pancreatic trypsin inhibitor. Biochemistry 1982;21:5230–5241.
31. Kitao A, Hirata F, Go N. The effects of solvent on the conformation and the collective motions of protein: normal mode analysis and molecular dynamics simulations of melittin in water and in vacuum. Chem Phys 1991;158:447–472.
32. Hayward S, Kitao A, Hirata F, Go N. Effect of solvent on collective motions in globular protein. J Mol Biol 1993;234:1207–1217.
33. Ansari A. Langevin modes analysis of myoglobin. J Chem Phys 1999;119:1774–1780.
34. Ermak DL, McCammon JA. Brownian dynamics with hydrodynamics interactions. J Chem Phys 1978;69:1352.
35. Takada S, Luthey-Schulten Z, Wolynes PG. Folding dynamics with nonadditive forces: a simulation study of a designed helical protein and a random heteropolymer. J Chem Phys 1999;110:11616–11629.

 DOI 10.1002/prot